International Journal of Cardiology 201 (2015) 595–600

Contents lists available at ScienceDirect

International Journal of Cardiology

journal homepage: www.elsevier.com/locate/ijcard

The Thebesian valve height/coronary sinus ostium diameter ratio (H/D-Ratio) as a new indicator for specifying the morphological shape of the valve itself in multisliced computed tomography

Wiesława Klimek-Piotrowska [a,1], Mateusz Koziej [a,1,*], Mateusz K. Hołda [a,1], Kinga Sałapa [b,1], Marcin Kuniewicz [a,c,1], Jacek Lelakowski [c,1]

[a] Department of Anatomy, Jagiellonian University Medical College, Cracow, Poland
[b] Department of Bioinformatics and Telemedicine, Jagiellonian University Medical College, Cracow, Poland
[c] Department of Electrocardiology, Institute of Cardiology, The John Paul II Hospital in Cracow, Jagiellonian University Medical College, Cracow, Poland

ARTICLE INFO

Article history:
Received 29 May 2015
Received in revised form 13 August 2015
Accepted 19 August 2015
Available online 24 August 2015

Keywords:
Coronary sinus
Multisliced computed tomography
Cardiac resynchronization therapy

ABSTRACT

Background: The coronary sinus ostium (CSO) is covered by the Thebesian valve (ThebV), which has a variable shape when assessed subjectively. The ThebV is an anatomical barrier during CS cannulation, which may be complicated due to the valves' size. The types of valves are: cord, remnant, semilunar, fold, and mesh/fenestrated. The ThebV can be visible using multisliced computed tomography (MSCT), however, this method cannot show the ThebV's morphological shape, only its size.

Methods: 301 randomly selected autopsied human hearts were examined. The shape of the valve was subjectively assessed, whereas the ThebV height (H) and the CSO diameter (D) were measured. The H/D-Ratio was computed as the ThebV height divided by the CSO diameter, afterwards k-means cluster analysis was performed to estimate H/D-Ratio's range of values between valves. MSCT scans from 114 patients that underwent CSO cannulation were objectively evaluated based on similar measured parameters in accordance with received H/D-Ratio values.

Results: Boundaries of ratio evaluations between remnant and semilunar, and semilunar and fold types were 0.35 and 0.65 respectively. In MSCT scans, the ThebV was recorded in 61 cases (remnant = 5.3%, semilunar = 24.6%, fold = 16.7%, cord = 0.0%, mesh/fenestrated = 7.9%). Except for the remnant and cord types, the other types appear similarly as in the cadaveric and MSCT studies. There were no differences between ThebV height and the CSO diameter in cadavers and MSCT studies.

Conclusion: The H/D-Ratio can be useful in assessing ThebV shape as visualized in MSCT. We give threshold values for the H/D-Ratio which easily allow the ThebV shape to be determined.

1. Introduction

The valve of the coronary sinus ostium (CSO), the so-called Thebesian valve (ThebV), is a structure that separates two cavities: the CSO and right atrium. The CSO is a target for many medical procedures, such as: cardiac resynchronization therapy (CRT), mapping and catheter ablation of cardiac arrhythmias, defibrillation, perfusion therapy, mitral valve annuloplasty, targeted drug delivery, retrograde cardioplegia administration [1–4] and diverse coronary blood flow [5,6]. Acting like a "guard dog", the leaflet of this valve can pose difficulties in cannulation of the coronary sinus (CS) [7]. In approximately 2.5% of cases, the presence of the obstructive ThebV can be a cause of unsuccessful CS cannulation [8]. This explains why more studies on the valve are needed to provide the necessary knowledge for clinicians.

ThebV is quite variable in shape and in earlier studies on autopsied hearts we have proposed a classification based on ThebV morphology [8]: remnant (type I — small hem of endocardium which does not significantly protrude into the lumen of the CSO), semilunar (type II — significantly protruding valve with a characteristic semilunar shape of the free edge), fold (type III — almost completely covering the whole CSO), cord (type IV — single thick strand of the endocardium, mostly localized midline) and mesh/fenestrated (type V — fenestrated valves in shape from I to III type; net-like valves and multiple cords).

So far, there have been numerous articles published on this topic involving studies performed on cadavers [9,10] and a few in computed tomography (CT) [11–13]. However, there is not enough detailed research which presents classification of ThebV in CT, which provides reference for the anatomical profile of the valve. In every cadaveric study the shape of the valve is assessed subjectively. Our aim was to

* Corresponding author at: Department of Anatomy, Jagiellonian University Medical College, Kopernika 12, 31-034 Cracow, Poland.
E-mail address: katedra.anatomii@gmail.com (M. Koziej).

[1] This author takes responsibility for all aspects of the reliability and freedom from bias of the data presented and their discussed interpretation.

http://dx.doi.org/10.1016/j.ijcard.2015.08.144
0167-5273/

find a method that allows the assessment of the true ThebV morphology in an objective way using CT imaging. Thus, we took classification from the study on cadaver specimens and used it in a multisliced computed tomography (MSCT) study and compared both. We believe, that our study could provide a very helpful tool for clinicians who perform CS cannulation.

2. Material and method

Methodology of the present research was done in accordance with the scheme presented in Fig. 1.

2.1. Study population

The cadaveric part of the study was conducted by the Department of Anatomy at the Jagiellonian University Medical College in Cracow, Poland. The presence of the coronary sinus ostium and the ThebV was examined in 301 autopsied human hearts of both sexes (234 (77.7%) men, 67 (22.3%) women), aged from 18 to 94 years old (48.6 ± 15.2 years). Specimens were collected during routine forensic medical autopsies performed at the Department of Forensic Medicine, Jagiellonian University Medical College. The study was approved by the Bioethical Committee of the Jagiellonian University Medical College, Cracow (no. KBET/51/B/2013). The study protocol conforms to the ethical guidelines of the 1975 Declaration of Helsinki. After dissection, all hearts were fixed in 10% formalin for a maximum of two months up to the time of measurement.

The CT scan analysis was performed on patients who underwent CSO cannulation to CRT in the Department of Electrocardiology, Jean Paul II Hospital, Jagiellonian University Medical College in Cracow, Poland. The study sample consisted of 114 patients (83 (72.8%) men, 31 (27.2%) women), aged from 29 to 86 years old (62.6 ± 11.8 years); average ejection fraction (EF) = 34.6 ± 17.5 ml.

2.2. Dissection and measurements of cadavers

All 301 heart specimens were opened in the standard routine manner by an incision extending from the orifice of the SVC to the orifice of the IVC. The CS was opened longitudinally along its free wall to allow easy measurement of the diameter of the CSO without damaging the ThebV. All descriptions and measurements were undertaken with the heart held in anatomical position and started with subjective assessment of the shape of a valve (type I–V). From all of the hearts' data samples, only 3 types of valve were taken into account for further calculation, these are: the remnant, the semilunar and the fold. The reason for choosing these shapes is the fact that they are quite regular in shape (arise from the same place — the atrial wall), unlike the cord and mesh/fenestrated types which shapes are irregular and difficult to predict.

The following measurements were made: the height of ThebV (H) and diameter of the CSO (D) (Fig. 2A). All measurements were conducted by 0.03 mm precision electronic caliper YATO (YT-7201). Measurements were performed twice to reduce the chance of error. The mean of the two measurements was calculated rounding to the one decimal place. The ThebV valve height measurements were taken between the free edge of the valve and its attachment site to the right atrium as the shortest dimension passing through the middle of the free edge parallel to the transverse diameter of the CSO. The transverse diameter of the CSO was measured through the incision in the CS as the largest dimension up to the first point of resistance.

2.3. Calculating the new indicator

For this study H/D-Ratio was computed by the following method: the height of the ThebV divided by the CSO diameter (Fig. 2B). Only valves from shapes I to III (remnant, semilunar, fold) were included in further analysis. Because of its morphology, the height of types IV (cord) and V (mesh or fenestrated) were not measured. Valves with the H/D-Ratio higher than 1 (max 1.54) from cadaveric sample (5 cases) were similarly excluded from further analysis of marking out the boundaries. These valves covered the whole CSO and their free edges significantly extended beyond the CSO contour.

2.4. Cardiac CT protocol

Before the cardiac CT examination procedure, every patient had their pulse checked. If the heart rate was over 70 bpm, the patient was administrated 10 or 40 mg of propranolol or 40 mg verapamil according to medical indications. The CT was performed using a 64-row dual-source scanner (Somatom Definition, Siemens, Erlangen, Germany). The contrast enhanced ECG-retrospectively gated image acquisitions were performed during inspiratory breath hold. The imaging parameters for dual-source CT were tube voltage of 100–120 kV and effective tube current of 350–400 mA. The collimation and temporal resolution revealed 2 × 32 × 0.6 mm and 165 ms. The arrival time of contrast agent to the ascending aorta was determined at the level of the carina with the use of a test bolus method (volume of 15 ml contrast agent, followed by 20 ml saline). Contrast agent was injected at the dose of 1.0 ml/kg and a rate of 5.5 ml/s followed by 40 ml saline chaser at the same rate range. The acquisition delay was the time of maximum density of the ascending aorta in the test bolus with additional 6 s of delay. Images were reconstructed with a B26f and B46f kernel and an image matrix of 512 × 512 pixels. Multiphase reconstruction (from 10% to 100%) was done and the best quality image reconstructions were assessed. The post-processing and study evaluation were performed using a dedicated workstation (Aquarius, TeraRecon, San Mateo, United States) by an experienced radiologist. Multiplanar (MPR) and volume rendered technique (VRT) reconstructions were used to identify CS ostium in Ludinghausen modifications, number and variety of veins over the left ventricle, distances and angles between branches of CS.

2.5. Multisliced computed tomography (MSCT) measurements

The ThebV was analyzed in accordance with anatomical classification. The presence of the valve was checked, its height (portion which protrudes into CSO) was measured as well as its CSO diameter (Fig. 2A). Measurements were performed by two researchers independently using virtual calipers, mostly during the phase 70% in axial projection.

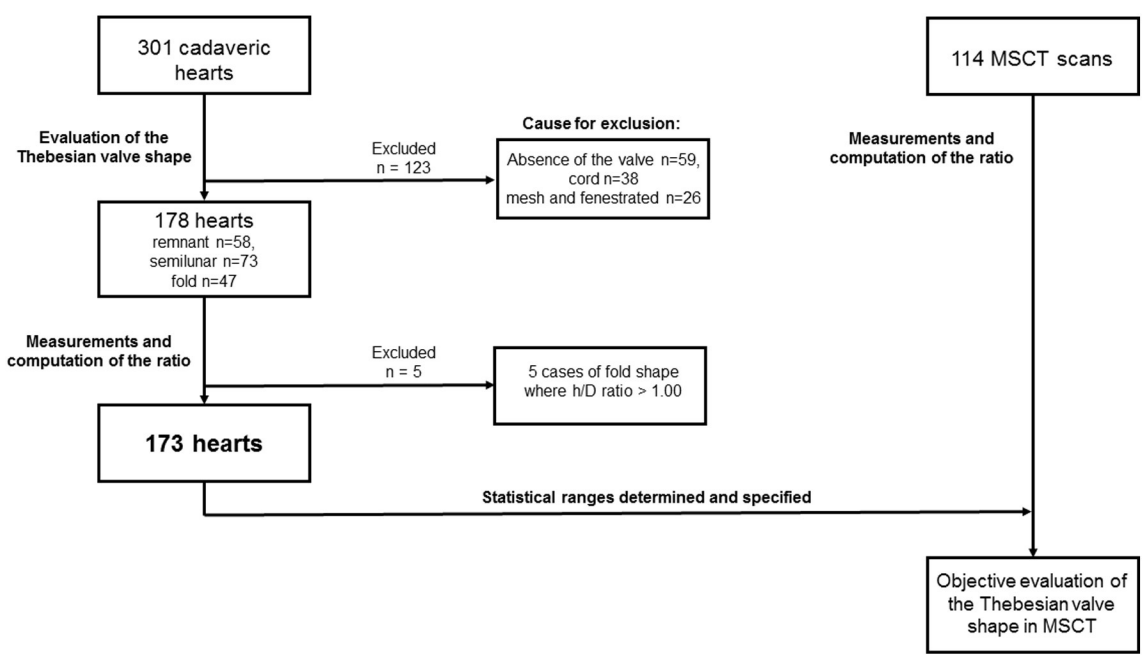

Fig. 1. Flow-chart with the study methodology. Using anatomy classification of the valve on cadaver samples, the H/D-Ratio was computed (the Thebesian valve height divided by the coronary sinus ostium). After that, statistical boundaries were specified which allowed to evaluate in an objective way the shape of the ThebV in the CT scans. MSCT — multisliced computed tomography.

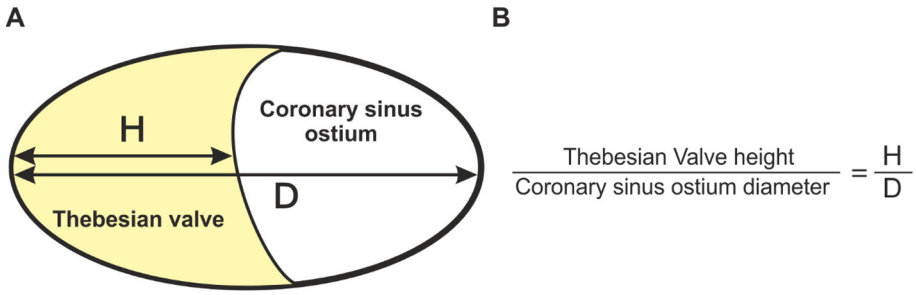

Fig. 2. (A) The method of measurements of the Thebesian valve (ThebV) height and the coronary sinus ostium (CSO) diameter. (B) The H/D-Ratio was computed as the ThebV height divided by the CSO diameter.

This allowed a way to calculate parameters of the H/D-Ratio which were comparable with those calculated on corpses. The average score of two values was taken. The valve was seen as a hypo-dense structure, that was prominent into the CSO. Additionally, differences in the contrast distribution between the CS and right atrium were observed when the valve was present. The ThebV was classified as either remnant, semilunar or fold according to its relative size. Also the presence of fenestrations within the valve could be seen (as differences in density and contrast leakage through fenestrations). If that appeared, the valve was classified into the mesh/fenestrated group.

2.6. Statistical analysis

Quantitative features were usually characterized using the mean value ± standard deviation. Quantiles (Q1, Me, Q3) were applied if non-parametric test was performed to compare quantitative features in groups. Minimum and maximum values were added in both cases. Qualitative features were presented by frequencies and percentages.

The Shapiro–Wilk test was applied to determine if the quantitative data were normally distributed. To verify homogeneity of variance the Levene's test was performed. Comparisons of average values of selected features in the cadaver and CT groups (Table 2) were performed using t-test for two groups. Otherwise, the data were analyzed using non-parametric Mann–Whitney test in the absence of normality or Welch's test in the absence of homogeneity of variance, respectively. Bonferroni correction was applied because of multiple comparisons. To control the I type error rate at 5%, the individual hypothesis was tested at a significance level of 1/m, where m is equal to 13 (Table 2). Hence, the individual significance level is 0.004.

The cluster analysis using generalized k-means algorithm with v-fold cross-validation was performed to sort different objects into groups so that the degree of association between two objects is maximal if they belong to the same group, and minimal otherwise. Input data into the cluster analysis came from the results of H/R-Ratio. The general purpose of the v-fold cross-validation algorithm is to divide the whole dataset into random v samples. Cluster analysis is performed using a training sample created by observations belonging to v-1 folds, and then the results are applied to a testing sample (the rest of the data) to compute an index of predictive validity. These calculations were repeated v times. Next, the results of v replications are averaged to yield a single measure of model stability. Squared Euclidean distance was used as distance metrics. The statistical analyses were performed with STATISTICA v10 (StatSoft Inc., Tulsa, OK, USA). p-Value of <0.05 was considered to be statistically significant.

3. Results

3.1. Cadaveric study

The valve was observed in 242 (80.4%) of cases (Table 1). The frequencies of groups needed for the H/D-Ratio analysis were: the remnant — type I n = 58 (19.3%), the semilunar — type II n = 73 (24.3%) and the fold — type III n = 47 (15.6%) (Fig. 1). The analyzed types (I–III) accounted n = 173 (58.3%) of all investigated hearts. The overwhelming majority of the ThebVs took its origin from the right margin of the CSO then further extending on its caudal and cranial edge. We noted that the ThebV was never attached to the left margin of the CS orifice.

The median H/D-Ratio values in the cadaveric specimens were 0.21, 0.58 and 0.78 for types I–III of the ThebV, respectively (Table 2). The median CSO (14.00 mm) diameter was the largest in the remnant type. Between each of the groups there was no clear border in the H/D-Ratio parameter.

3.2. Counting the boundaries

Fig. 3 presents the described model, where k-cluster analysis between groups was evaluated and the area between intersectional groups is illustrated. Mentioned area is larger between types II and III, which means that those types during subjective evaluation overlap the most in the value for the H/D-Ratio.

Following study methodology, we computed intervals of H/D-Ratio for each group (Fig. 4):

- I — remnant: (0.00–0.35 > average 0.22
- II — semilunar: (0.35–0.64) — average 0.52
- III — fold <0.64–1.00) — average 0.77.

3.3. MSCT study

According to the above intervals and anatomy classification, a morphology of the ThebV in the CT was described (Fig. 5). MSCT study results are shown in Table 1. ThebV was recorded in 62 cases (54.4%). The remnant (I) was observed only in 6 (5.3%) cases. The semilunar (II) type was the most frequent type of valve (24.6%). The fold (III) was found in 19 cases (16.9%). The cord (IV) was not recorded and mesh/fenestrated (V) was observed in 9 hearts (7.9%). The absence of the valve was noticed in 52 (45.6%) cases of the MSCT study sample. Values of median H/D-Ratio obtained from CT measurements were 0.30, 0.46 and 0.77 respectively for the I–III types (Table 2). Mean value of the CSO diameter in the whole CT data sample were 11.9 ± 3.6 mm.

3.4. Study comparison

Occurrence of remnant (type I) shape was different between study groups in contrast with the rest of the shapes where the frequencies were similar (Table 1). The absence of the valve was much more frequent in the MSCT group. The H/D-Ratio was significantly higher ($p < 0.004$) in the cadaveric study in the semilunar (II) type of valve (Table 2). No significant differences were noted in the ThebV's height

Table 1
Occurrence of different types of the Thebesian valve in cadavers and in multisliced computed tomography (MSCT) study patients with comparison between groups.

	Type	Cadavers (n = 301)		MSCT (n = 114)	
		n	%	n	%
	Absence	59	19.6%	52	45.6%
I	Remnant	58	19.3%	6	5.3%
II	Semilunar	73	24.3%	28	24.6%
III	Fold	47	15.6%	19	16.7%
IV	Cord	38	12.6%	0	0.0%
V	Mesh and fenestrated	26	8.6%	9	7.9%

Table 2
Statistical values [mm] of measurements done on cadavers and multisliced computed tomography (MSCT) scans with computed ratio.

	Cadaver study (n = 301)						MSCT study (n = 114)						p*
	Thebesian valve height (H)						Thebesian valve height (H)						
	n	Median	Q1	Q3	Min	Max	n	Median	Q1	Q3	Min	Max	
Remnant	58	3.00	2.08	3.00	0.30	4.20	6	3.40	2.70	3.70	2.30	5.20	0.2094
Semilunar	73	6.26	5.00	8.00	2.18	11.00	28	5.05	4.10	7.00	3.00	12.30	0.0427
Fold	42	8.00	6.25	10.00	1.59	13.00	19	9.30	7.50	10.40	2.70	17.30	0.1103
Total	173	5.00	3.00	8.00	0.30	13.00	53	5.70	4.20	8.90	2.30	17.30	0.0285
	Coronary sinus ostium diameter (D)						Coronary sinus ostium diameter (D)						p
Remnant	58	14.00	9.66	15.00	4.50	18.00	6	12.00	10.60	14.60	7.50	15.60	0.5116
Semilunar	73	12.00	9.00	13.00	4.16	16.00	28	10.50	9.20	13.90	6.60	21.50	0.8981
Fold	42	10.00	8.70	12.00	2.06	15.00	19	11.60	10.20	13.20	6.30	17.40	0.0659
Total	173	12.00	9.00	14.00	2.06	18.00	53	11.50	9.50	13.90	6.30	21.50	0.8345
	H/D-Ratio						H/D-Ratio						p
Remnant	58	0.21	0.18	0.25	0.03	0.44	6	0.30	0.29	0.33	0.17	0.36	0.0262
Semilunar	73	0.58	0.50	0.68	0.29	0.86	28	0.46	0.41	0.56	0.37	0.65	0.0001
Fold	42	0.78	0.74	0.83	0.55	0.98	19	0.77	0.71	0.86	0.28	1.00	0.8655
Total	173	0.55	0.25	0.71	0.03	0.98	53	0.54	0.41	0.72	0.17	1.00	0.2103
	Coronary sinus ostium diameter when absent of valve						Coronary sinus ostium diameter when absent of valve						p
Absence	59	16.00	12.48	17.00	4.60	18.00	52	12.65	9.15	15.55	3.80	20.40	0.0003

Q1 and Q3 — lower and upper quartiles.
H/D-Ratio — Thebesian valve height (H) divided by coronary sinus ostium diameter (D) in the remnant, the semilunar and the fold types, respectively.
* Results are considered statistically significant at $p < 0.004$ to allow for a Bonferroni correction accounting for the multiple comparisons.

and the CSO diameter between studies in the remnant (I), semilunar (II) and fold (III) types. However, in groups where the ThebVs were absent the CSO diameter was higher in the cadaveric study.

4. Discussion

The present research shows how the anatomical knowledge based on specimens was put into the clinical description by the CT. The authors propose an indicator based on statistical algorithms which in the MSCT acts in the same way as it does on the cadaver specimen. The MSCT is a very helpful tool which allows easy visualization of the ThebV and may provide detailed information for the CS cannulation procedure, particularly for valve variations that can potentially affect the approach to CRT [13,14]. Furthermore, optimal imagining of the CS with its tributaries is essential to minimize procedural morbidity and improve CRT long-term success.

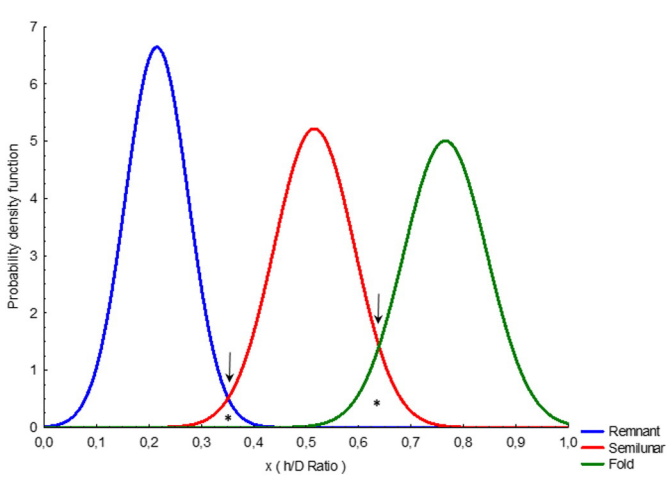

Fig. 3. Distribution of H/D-Ratio for the remnant, the semilunar and the fold type of the Thebesian valve on a horizontal axis during k-cluster method analysis. Each type is generated as probability density function which corresponds with the number of density cases where the top equals with the average value of the H/D-Ratio and the tail refers to the range. Particular sets overlap, that area (*) is larger between the semilunar and the fold types. Intersections between sets define boundaries: 0.35 and 0.64 (arrows).

For authors, the best knowledge, this is the first study which compares ThebV height and CSO diameter between post-mortem specimens and MSCT patients. The methodology of measurements in every study was analogous and comparable (the same plane of measurements was preserved). Additionally, both cadaveric and MSCT studies were performed by the same investigators. The sample of the paper is the largest up to date.

The presence of the ThebV may determine the possibility of CS cannulation [15]. Only two types of vales: fold and mesh/fenestrated (16.7% and 7.9% respectively in MSCT study) are believed to make cannulation difficult, sometimes even impossible [16]. In CT data samples the occurrence of those types was accounted in total of 24.6%. The study shows that the appearance of those two types was quite similar with cadaveric study after using H/D-Ratio. It highlights how the noninvasive examination can be useful in selecting an appropriate method of treatment. The proposed method of ThebV assessment reflects an essential reality for CS cannulation cases.

Valves classified as a types I — remnant, II — semilunar, and IV — cord of their size and location probably have no influence on CS cannulation. In the CT sample some of the remnant (5.3%) and cord (0.0%) shapes were less frequent than in the cadaveric study (respectively: 19.3% and 12.6%). An explanation may be due to the fact that these structures are very thin and couldn't be recorded in the CT. In cadaveric specimens

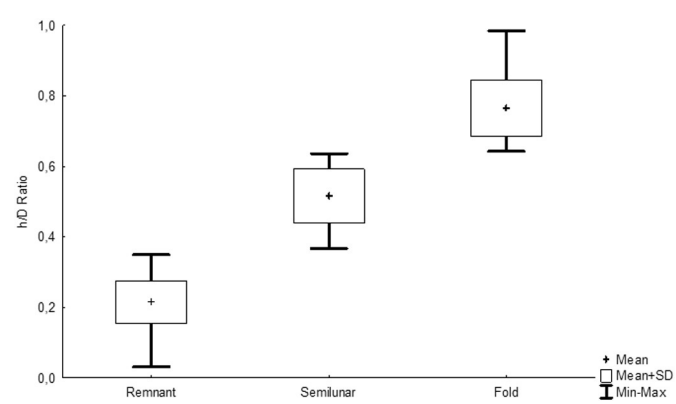

Fig. 4. Box-&-whisker plot which shows the means, SD and range for the remnant, semilunar and fold type of the Thebesian valve after k-cluster method analysis.

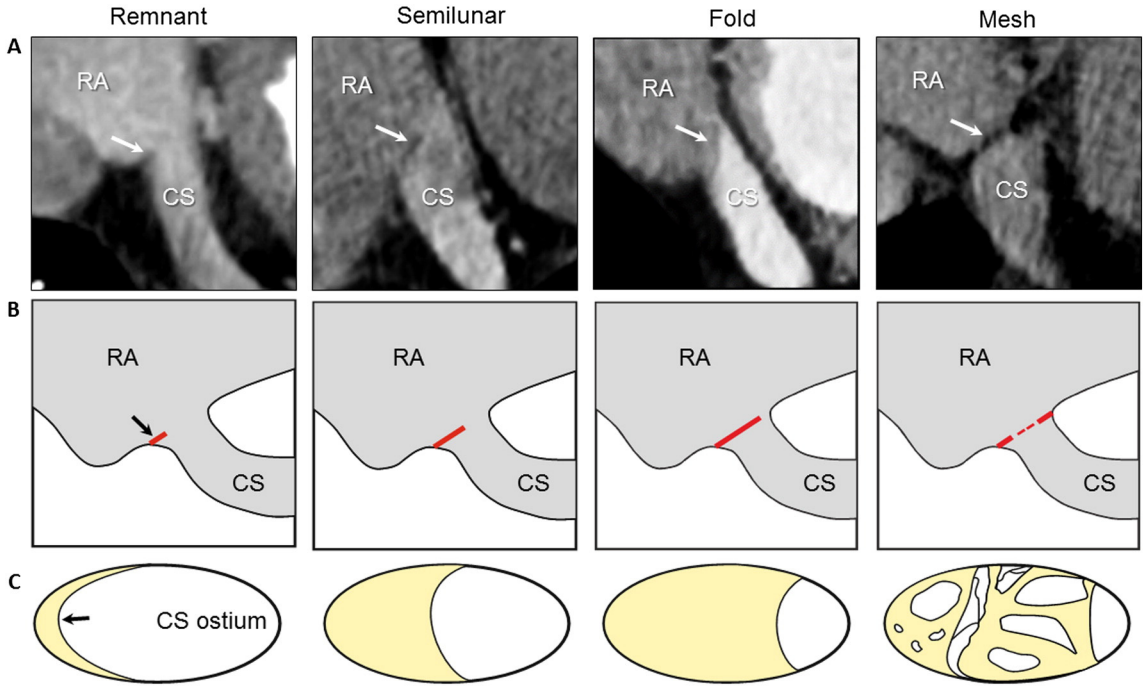

Fig. 5. Thebesian valve (arrow) types visualized in multisliced computed tomography (A) with schematic CT slice view (B) and theoretical anterior view (C). Shape is based on ThebV height (H) divided by coronary sinus (CS) ostium diameter (D) ratio, and classified according to the cadaveric study. Intervals of ratio for each type of valve: remnant (0.00–0.35>; semilunar (0.35–0.64); and fold - <0.64–1.00). Remnant (h: 3.1 mm; D: 10.6 mm; ratio: 0.29), semilunar (h: 7.6 mm; D: 15.6 mm; ratio: 0.49), fold (h: 12.2 mm; D: 12.2 mm; ratio: 1.00), mesh (D: 12.8 mm).

the average width of the cord is about 0.5–2.0 mm. Its course is usually irregular and plain slices are inadequate as our results have shown. To obtain the cord image, the authors suggest to make 3-dimension visualization using high quality equipment (however, this is not clinically relevant). The smallest detected remnant valve in CT by investigators had 2.3 mm and the smallest remnant case in corpses was 0.3 mm. We believe that every undetected valve from the two shapes mentioned (in total CT: 5.3%, cadavers: 31.9%, difference: 26.6%) could be due to an absence of the valve (CT: 45.6%, cadavers: 19.6%, difference 26.0%). As we mentioned, those shapes couldn't be an obstacle during CS cannulation and they have less clinical relevance.

Computed tomography is an invaluable diagnostic tool in the cardiovascular disease field, which helps in making a diagnosis, planning and performing invasive procedures, as well as assessing the effects of treatment [17–21]. The equipment used in present study is 64-row MSCT, probably the most commonly available in cardiologic centers. The use of that typical CT was intentional to show that despite all higher-row devises (such as 128, 256, 320 row CTs), 64 row CT was sufficient to visualize the ThebV. Our results and those from Mlynarski et al. [12] confirmed that this method allows assessment of the valve, in particular larger structures which can pose difficulties during CS cannulation and are clinically relevant. Technology advances may make these processes more accurate and will allow to generate images of higher quality and thus visualize even smaller structures, such as cords or remnants. Estimation of the ThebV can be done during routine cardiac tomography assessment of the CS tributaries. The results in this field are promising, Sun et al. [22] reported that 256-row MSCT can provide superior noninvasive evaluation of the coronary venous system.

Next, the results of this study were compared with other available publications, but the number of publications which assesses the real shape of the ThebV in CT is limited. Malagò et al. [23] performed their research on 301 hearts in 64-slice CT and found ThebV in 77% of cases. The mean value of CSO diameter in their study was 8.7 mm (no SD given). In the study performed on 339 hearts in 128-row CT by Berhan Genc et al. [24], Theb valve was recorded in 72.2% but their appearance wasn't described. The CSO diameter was 9.5 ± 2.1 mm. Mao et al. [25] have conducted their study using the Electron Beam Computed Tomography (EBCT). Although they didn't evaluate ThebV occurrence, they measured the CSO diameter (10.5 ± 2.4 mm). Similarly the study by Chiribiri et al. [26] performed in the cardiac MRI on 23 patients, where average CSO diameter was 11.0 ± 3.6 mm, did not check the valve shape. Evaluation of the CS venous system was also performed on 16-row MSCT. In the study by Jongbloed et al. [27] carried out in 16-row MSCT the diameter of the CSO was 12.6 ± 3.6 mm in the anteroposterior direction.

Christiaens et al. [11] conducted measurements of the ThebV on 50 patients and reported valve in 36% (n = 18) of cases. Moreover, the ratio between the ThebV area and the ostium area was checked (presented as %): 20% (2 patients); 30% (10 patients); 50% (5 patients); and 60% (1 patient). The ThebV was always in the posteroinferior side of the CSO. Rewriting these results using our classification 20% and 30% ratio valves are the remnant (I) type (12/50 = 24%); 50% and 60% ratio valves are the semilunar (II) type (6/50 = 12%). No valve meets the criteria for the fold (III) type.

Mlynarski et al. [12] in their 64-row MSCT study have presented valve classification (7 types: A1, 2, B1, 2, C, D, E) according to: place of divergence, number of visible parts and diameter of membrane (n = 199). According to their study, in 46% of cases ThebV was observed. They checked also whether the valve started from the interatrial septum or wall of the atrium. We made an attempt to compare our MSCT results with Mlynarski [12] but these classifications are not fully corresponding. The remnant (I) and semilunar (II) types of valve from our classification could be classified as A1 (membrane covers less than 50% of CSO visible from the atrium wall), fold (III) type as A2 (membrane covers more than 50% of CSO visible from the atrium wall) or D (whole ostium is covered) and mesh/fenestrated (V) type as a E (the whole CSO is covered by porous membrane).

In this cadaver study we noticed, that the ThebV in types I–III (remnant, semilunar, fold) is always attached only to the atrium wall (right inferior CSO circumference). Interestingly Mlynarski at al. reported valves which were visible from the interatrial septum side. We have a simple explanation for that. In some cases cords have irregular course and sometimes they are placed anteriorly to the CSO. A similar situation was in the case of mesh/fenestrated type, it had unpredictable shape

which occurs as a few strings forming a kind of thin network and often covered the entire ostium. Therefore we suggest that prominent structures seen from the interatrial wall could be the part of a crossing cord or mesh type of valve. The cord and mesh/fenestrated types may be roughly described as those visible from the interatrial septum B1 (membrane covers less than 50% of CSO), B2 (more than 50% of CSO), and C (built from two separate parts with a gap between).

The identification of the clinically significant ThebB valve is uncomplicated and can be done by a specialist without having much experience in the heart imaging. This is a fast method of visualization of the ThebV, which can give clear view of the situation before taking any procedure. Comprehensive knowledge of the cardiac anatomy from a CT perspective is essential for thoracic and cardiac imaging technicians [14]. That may help to choose an appropriate operation technique. When fold or mesh type of ThebV is observed, high risk of failure and complication can occur. Therefore, other therapeutic options or radiofrequency puncture may be taken into consideration [28,29]. We do not recommend performing a CT scan on every patient before undergoing CS cannulation, but to use the existing CT of the patient's heart when available.

The limitations of our study are very minor changes in the specimen's size after fixation in 10% formalin, and measurements of the heart regardless of the cardiac cycle on cadavers and insufficient CT resolution for imaging smaller structures such as cords or remnants. The patients' heart descriptions evaluated in CT were not confirmed in anatomopathological autopsy. In spite of all this, we believe that those factors are still insignificant to affect the study analysis. Further studies are needed to evaluate how each type of valve affects CS cannulation and has influence on the procedure outcome.

5. Conclusion

The H/D-Ratio can be useful in assessing the anatomical ThebV shape in the non-invasive MSCT. This study gives threshold values for the H/D-Ratio which easily allows determination of the anatomical ThebV shape which could help to choose the adequate technique and avoid complications during CS cannulation. Computed intervals of H/D-Ratio for each type of valve are: remnant = (0.00–0.35 > semilunar = (0.35–0.64); and fold = <0.64–1.00). There were not any differences between ThebV height and the CSO diameter in cadavers and MSCT studies. High quality equipment and 3-dimension reconstruction are needed to evaluate cords, mesh and the very thin remnant shape of ThebV.

Conflict of interest

The authors report no relationships that could be construed as a conflict of interest.

Acknowledgments

We sincerely thank Mr. Matthew Ficinski for helping us finalize this paper. His contribution to reviving this paper by checking for proper English grammar was very variable. We greatly appreciate his time and effort for helping us.

References

[1] J.C. Daubert, P. Ritter, H. Le Breton, D. Gras, C. Leclercq, A. Lazarus, J. Mugica, P. Mabo, S. Cazeau, Permanent left ventricular pacing with transvenous leads inserted into the coronary veins, Pacing Clin. Electrophysiol. 21 (1998) 239–245.
[2] E.N. Prystowsky, Diagnosis and management of the preexcitation syndromes, Curr. Probl. Cardiol. 13 (1988) 225–310.
[3] R. Cappato, M. Schlüter, C. Weiss, S. Willems, T. Meinertz, K.H. Kuck, Mapping of the coronary sinus and great cardiac vein using a 2-French electrode catheter and a right femoral approach, J. Cardiovasc. Electrophysiol. 8 (1997) 371–376.
[4] J.H. Spencer, S.E. Anderson, P.A. Iaizzo, Human coronary venous anatomy: implications for interventions, J. Cardiovasc. Transl. Res. 6 (2013) 208–217.
[5] H. Obata, H. Nishijima, H. Yasuda, experimental evaluation of the reliance of coronary sinus blood flow (CSF) and great cardiac vein blood flow (GCVF) measured by local thermodilution method, Hokkaido Igaky Zasshi 66 (1991) 161–169.
[6] J. Kaufmann, J.H. Gerds-Li, C. Kriatselis, E. Fleck, S. Goetze, Three-dimensional rotational venography of the coronary sinus tree facilitates left ventricular lead implantation for CRT, J. Interv. Card. Electrophysiol. 42 (2015) 125–128.
[7] J. Kautzner, Thebesian valve: the guard dog of the coronary sinus? Europace 11 (2009) 1136–1137.
[8] M.K. Hołda, W. Klimek-Piotrowska, M. Koziej, M. Mazur, Anatomical variations of the coronary sinus valve (Thebesian valve): implications for electrocardiological procedures, Europace 17 (2015) 921–927.
[9] S.K. Ghosh, S. Raheja, A. Tuli, Obstructive Thebesian valve: anatomical study and implications for invasive cardiologic procedures, Anat. Sci. Int. 89 (2014) 85–94.
[10] G.S. Mak, A.J. Hill, F. Moisiuc, S.C. Krishnan, Variations in Thebesian valve anatomy and coronary sinus ostium: implications for invasive electrophysiology procedures, Europace 11 (2009) 1188–1192.
[11] L. Christiaens, P. Ardilouze, S. Ragot, J. Mergy, J. Allal, Prospective evaluation of the anatomy of the coronary venous system using multidetector row computed tomography, Int. J. Cardiol. 126 (2008) 204–208.
[12] R. Mlynarski, A. Mlynarska, M. Tendera, M. Sosnowski, Coronary sinus ostium: the key structure in the heart's anatomy from the electrophysiologist's point of view, Heart Vessels 26 (2011) 449–456.
[13] J.S. Shinbane, M.J. Girsky, S. Mao, M.J. Budoff, Thebesian valve imaging with electron beam CT angiography: implications for resynchronization therapy, Pacing Clin. Electrophysiol. 27 (2004) 1566–1567.
[14] J.P. O'Brien, M.B. Srichai, E.M. Hecht, D.C. Kim, J.E. Jacobs, Anatomy of the heart at multidetector CT: what the radiologist needs to know, Radiographics 27 (2007) 1569–1582.
[15] M. Karaca, O. Bilge, M.H. Dinckal, H. Ucerler, The anatomic barriers in the coronary sinus: implications for clinical procedures, J. Interv. Card. Electrophysiol. 14 (2005) 89–94.
[16] A.J. Hill, J.A. Coles, D.C. Sigg, T.G. Laske, P.A. Iaizzo, Images of the human coronary sinus ostium obtained from isolated working hearts, Ann. Thorac. Surg. 76 (2003) 2108.
[17] K. Nakamura, N. Funabashi, S. Naito, M. Uehara, H. Takaoka, K. Kaseno, K. Kumagai, S. Oshima, Y. Kobayashi, Anatomical relationship of coronary sinus/great cardiac vein and left circumflex coronary artery along mitral annulus in atrial fibrillation before radiofrequency catheter ablation using 320-slice CT, Int. J. Cardiol. 168 (2013) 5174–5181.
[18] A.A. Mahabadi, M.H. Geisel, N. Lehmann, C. Lammerding, H. Kälsch, M. Bauer, S. Moebus, K.H. Jöckel, R. Erbel, S. Möhlenkamp, Association of computed tomography-derived left atrial size with major cardiovascular events in the general population: the Heinz Nixdorf recall study, Int. J. Cardiol. 174 (2014) 318–323.
[19] A.C. Lindsay, M. Sriharan, O. Lazoura, S.P. Padley, E.D. Nicol, M.B. Rubens, Multidetector computed tomography of congenital aortic abnormalities, Int. J. Cardiol. 172 (2014) 537–547.
[20] G.S. Kanaganayagam, A.T. Ngo, A. Alsafi, R. Kamanahalli, N. Sutaria, T. Mittal, B. Ariff, Ct coronary angiography in the investigation of chest pain—beyond coronary artery atherosclerosis; a pictorial review, Int. J. Cardiol. 176 (2014) 618–629.
[21] A.W. Leber, M. Kasel, T. Ischinger, U.H. Ebersberger, D. Antoni, M. Schmidt, G. Riess, V. Renz, A. Huber, T. Helmberger, E. Hoffmann, Aortic valve calcium score as a predictor for outcome after TAVI using the CoreValve revalving system, Int. J. Cardiol. 166 (2013) 652–657.
[22] C. Sun, Y. Pan, H. Wang, J. Li, P. Nie, X. Wang, H. Ma, F. Huo, Assessment of the coronary venous system using 256-slice computed tomography, PLoS One 9 (2014) e104246.
[23] R. Malagò, A. Pezzato, C. Barbiani, G. Sala, G.A. Zamboni, D. Tavella, R.P. Mucelli, Non invasive cardiac vein mapping: role of multislice CT coronary angiography, Eur. J. Radiol. 81 (2012) 3262–3269.
[24] B. Genc, A. Solak, N. Sahin, S. Gur, S. Kalaycioglu, V. Ozturk, Assessment of the coronary venous system by using cardiac CT, Diagn. Interv. Radiol. 19 (2013) 286–293.
[25] S. Mao, J.S. Shinbane, M.J. Girsky, J. Child, S. Carson, R.J. Oudiz, M.J. Budoff, Coronary venous imaging with electron beam computed tomographic angiography: three-dimensional mapping and relationship with coronary arteries, Am. Heart J. 150 (2005) 315–322.
[26] A. Chiribiri, S. Kelle, S. Götze, C. Kriatselis, T. Thouet, T. Tangcharoen, I. Paetsch, B. Schnackenburg, E. Fleck, E. Nagel, Visualization of the cardiac venous system using cardiac magnetic resonance, Am. J. Cardiol. 101 (2008) 407–412.
[27] M.R. Jongbloed, H.J. Lamb, J.J. Bax, J.D. Schuijf, A. de Roos, E.E. van der Wall, M.J. Schalij, Noninvasive visualization of the cardiac venous system using multislice computed tomography, J. Am. Coll. Cardiol. 45 (2005) 749–753.
[28] S.J. Worley, How to use balloons as anchors to facilitate cannulation of the coronary sinus left ventricular lead placement and to regain lost coronary sinus or target vein access, Heart Rhythm. 6 (2009) 1242–1246.
[29] M.G. Parikh, S.M. Halleran, S. Bharati, R.G. Trohman, Successful percutaneous cardiac resynchronization despite an occlusive Thebesian valve, Pediatr. Cardiol. 32 (2011) 1223–1227.